Heliyon 10 (2024) e31318

Contents lists available at ScienceDirect

Heliyon

journal homepage: www.cell.com/heliyon

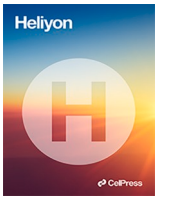

Research article

Hyperbranched polymeric membranes for industrial water purification

AmanyE. Taha [a], Salwa Mowafi [b], Asmaa S. Hamouda [c,*]

[a] *Environmental Sciences And Industrial Development Department, Faculty of Postgraduate Studies for Advanced Sciences (PSAS), Beni-Suef University, Egypt*
[b] *Proteinic and Man-made Fibers Department, Textile Research and Technology Institute, National Research Centre, 12622-Dokki, Giza, Egypt*
[c] *Associate Prof. of chemical and Environmental Enginnering, Environmental Sciences and Industrial Development Department, Faculty of Postgraduate Studies for Advanced Sciences (PSAS), Beni-Suef University, Egypt*

ARTICLE INFO

Keywords:
Polyacrylonitrile
Polyamide
Chitosan
Electro-spinning
Nano-fibers
Dual-layer nano-fibrous membrane
Adsorption of dye and heavy metal

ABSTRACT

This work aims at the preparation and characterization of dual-layer (DL) nano-fibrous mat (NFM) of hydrophobic and mechanical stable polyacrylonitrile (PAN) nano-fibers (NFs), as a supporter, and polyamide 6 (PA)/chitosan (Ch) NFs as a top hydrophilic coating layer.

PAN and PA fibers, as residual wastes from textile processes, were collected and dissolved in their proper solvents. PAN was electro-spuned under certain conditions of electro-spinning (voltage, flow rate, and distance between spinneret and collector) to obtain PAN-NFM. Different ratios of PA/Ch composite were prepared and then electro-spun above the PAN-NFM that was previously prepared to obtain hydrophobic/hydrophilic functional dual-layer nano-fibrous membrane (DLNFM). The efficiency of the prepared DLNFM for capturing dye residues and heavy metals from wastewater was investigated.

The viscosities of the prepared composite solutions were measured. The prepared dual-layer nano-fiber membranes (DLNFMs) were chemically and physically characterized by Fourier transform infrared spectroscopy, scanning electron microscope, X-ray diffraction, and thermogravimetric analyzer. The potential of the prepared mats for the adsorption of some heavy metal ions, i.e., Cu^{+2}, Cr^{+3}, and Pb^{+2} cations in addition to dyes from wastewater was evaluated. The effect of using different concentrations of PA/Ch composite as well as the thickness of the obtained DLNFM on the filtration efficiency was studied.

The results of this study show the success of functional DLNFM in dye and heavy metal removal. The maximum removal efficiency of acid dyes was reached to 73.4 % and of reactive dye was approximately 61 % for PAN/PA-1.25%Ch DLNFM after 3 days at room temperature. The removal efficiency percent of heavy metal ions reached to 54 % by DLNFM. Additionally, the results showed that 0.08 mm is the ideal thickness for maximum absorption capacity. This value is correlated with the membrane's highest Ch percentage, which is (PAN/PA-1.25%Ch). Furthermore, the results demonstrate that the presence of the Ch polymer strengthened the produced bi-layered membrane to achieve the highest thermal stability when compared to the other nano-fibrous membranes (NFMs), with the breakdown temperature of the Ch functionalized dual-layer membranes (DLMs) reaching approximately 617 °C and a maximum weight loss of 60 %.

* Corresponding author.
E-mail addresses: monymero137@gmail.com (AmanyE. Taha), ibrahimesalwa82@yahoo.com (S. Mowafi), Asmaa_hamouda@yahoo.com, Asmaa_hamouda@psas.bsu.edu.eg (A.S. Hamouda).

https://doi.org/10.1016/j.heliyon.2024.e31318
Received 21 February 2024; Received in revised form 18 April 2024; Accepted 14 May 2024
Available online 27 May 2024

1. Introduction

Wastewater effluent from several industries i.e., textile, dyes manufacturing, paint, pesticide, petroleum purifying, paper, timber,

Abbreviation

°C	Celsius
Ch	Chitosan
Cm	Centimeter
Cp	Centipoise
Cr^{+3}	Chromium III
Cu^{+2}	Copper II
DL	Dual-layer
DLM	Dual-layer mat
DLMs	Dual-layer mats or membranes
DLNF	Dual-layer nanofiber
DLNFM	Dual-layer nano-fibrous mat or membrane
DLNFMs	Dual-layer nano-fibrous mats or membranes
DMF	Dimethyleformamide
DSC	Differential scanning calorimetry
FT-IR	Fourier transform infrared spectroscopy
G/l	Gram per litter
gms	Grams
hr	Hour
Kg/cm2	Kilogram per square centimeter
kv	Kilo volte
ml	Milliliters
mm/s	Millimeters per second
NF	Nanofiber
NFM	Nano-fibrous mat or membrane
NFMs	Nano-fibrous mats or membranes
NFs	Nanofibers
Nm	Nanometer
PA	Polyamide
PAN	Polyacrylonitrile
Pb^{+2}	Lead
PH	Potential of Hydrogen
Ppm	Parts per million
Rpm	Revolution per minute
SEM	Scanning Electron Microscopy
Tg	Glass transition temperature
TGA	Thermogravimetric Analysis
Tm	Melting temperature
% W/V	g of solute/100 mL of solution
XRD	X-ray diffraction

pharmaceutical, mining, pulp, and plastics is polluted by various dyes and heavy metals which are carcinogenic, non-biodegradable, and contaminating for freshwater [1]. On the other hand, the typical treatment methods are not efficient enough due to technical and economic reasons. So, different techniques have been developed for the removal of dyes and toxic metals from wastewater before their discharge into the aquatic streams [2]. Membranes are the main of great interest for effluent treatment due to they do not need any addition of chemical agents [3].

Membrane technology plays an important role in securing global water [4]. This is due to its great efficiency, cost-effectiveness, and efficacy when it comes to treating various types of water sources to achieve the required quality of water. Membrane materials can be classified into two types, i.) inorganic or ceramic membranes, and ii.) organic or polymeric membranes) [5]. Polymeric membranes are generally cheap, simple to manufacture, and come in a variety of pore sizes, therefore they've been widely used in various fields [5].

Polymeric membranes are the most readily accessible on the market; however, they still have issues with fouling, deterioration, and general stability [6]. As a result, there has been a wave of studies into increasing the performance of polymeric membranes by modifying their design, structure, and physicochemical characteristics [5].

Membranes are mostly used in separation procedures in the chemical processing industry. These processes include microfiltration, ultrafiltration, reverse osmosis, electrodialysis, gas separation, Pervaporation, and facilitated transport. Different research groups investigated several approaches to enhance the properties and performance of membranes, which include: (i) incorporation of NFs in the polymeric matrix to form a mixed matrix membrane [7]; (ii) surface modification by the use of coatings and post-treatments [8]; (iii) fabrication of DL or triple-layer membranes; (iv) synthesis of new materials, and; (e) fabrication of engineered membrane structure with remarkable properties. Recently, researchers fabricated many advanced membranes [9,10] and NFs membranes [11–13] with different number of layers, with better texture, to achieve better properties that are required for water purification [14].

Electro-spinning is one of the best nano-fiber (NF) production technologies, as it has many advantages of a large variety of available raw materials, good porosity, small fiber diameter, and an easy process [15]. This spinning method requires electrostatic forces to create fine fibers from polymer solutions or melts [16].

NFs are described as fibers with a length-to-thickness ratio of less than 1000:1 [17]. Because of their unparalleled physicochemical features and qualities, NFs have appeared as attractive one-dimensional nanomaterials for a wide range of commercial and research applications [2]. These applications include energy generation and storage [18], biomedical [19]and tissue engineering [20], sensors [21] and catalysts [22], air/liquid filtration [23], drug delivery [24], and textiles [25].

PAN is an aliphatic polymer that consists of interconnected carbon chains through Nitrile polymerization [26]. PAN has been selected as the material for obtaining electro-spun NFs due to it has good mechanical and thermal stability. PAN-NFhas been widely used for microfiltration, ultrafiltration [27], nano-filtration [28], and reverse osmosis [29].

Ch, marine-based biomaterials, is a polysaccharide derivative [30], that has been applied to remove organic and inorganic pollutants such as (medicines, pesticides, dyes) and (heavy metal ions, phosphates, and fluoride), respectively through biosorption, adsorption, coagulation, reduction, or oxidation [31]. Ch is insoluble at neutral pH conditions and is water-resistant but water-permeable [32]. Ch is a highly promising substitute frequently utilized in producing polymeric membranes because of its availability, renewability, low environmental impact, and superior absorption [33–35].

Ch-based membranes have been the subject of extensive research in the past few years for extracting and absorbing organic dyes and heavy metal ions from wastewater. In its molecular chains, Ch has a large number of active functional groups, including hydroxyl and amino groups. This allows it to chelate cationic dyes and positively charged metal ions to form stable complexes. It can also use electrostatic contact to absorb negatively charged metal acid ions [36]. Consequently, a great deal of research has been done recently on Ch-based membranes for the removal and absorption of organic colors and heavy metal ions from wastewater. An adsorptive Ch membrane that was created to remove Rhodamine B dye from water was reported by Gharbani et al. with a rejection rate of 72.47 % [37]. Huo et al. produced acid-resistant composite membranes based on Ch that were extremely effective and selective in eliminating harmful anionic dyes from wastewater [38]. Using the film casting approach, Long et al. created positively charged Ch nano-filtration membranes that improved the removal of colors and salts from textile water. Because of their appropriate thickness and tensile strength, the as-fabricated Ch membranes demonstrated significant water permeate flow as well as excellent filtration capacities for popular colors and salts [33]. Unfortunately, the majority of these Ch-based membranes are made using chemical cross-linking or solvent-casting techniques, which typically produce membrane microstructures that are difficult to control, including porosity, roughness, pore size, and thickness. As a result, the potential to further improve Ch membrane water flux and separation accuracy is constrained. As such, the development of a flexible and versatile technique for the synthesis of enhanced Ch membranes with higher performance in dye/heavy metal separation is very desirable.

PA has excellent chemical and thermal resistance. It is usually dissolved in formic acid from which it can be easily electro-spun into NFs. The utilization of electro-spun PA NFMs as filtration materials has been reported [39]. PA-NFMs have poor dimensional stability and low mechanical properties as well as easily contract after water immersion which limits their applications in the filtration field. Recently, several techniques have been developed to overcome the mechanical weakness of NFs [40].

The DLMs are made up of two layers created by concurrently co-extruding or co-casting two distinct solutions followed by thermal lamination and heat press process [41]. With advancements in the DL concept, it is now possible to create membranes with maximum performance from a variety of polymeric pairings for liquid-phase and gas-phase separations [41]. The electro-spun DLNFMs had high porosity, excellent distribution for pore size, and extremely hydrophobic rough surfaces [41].

Due to the unique benefit of designing the functionality of the two layers separately, a large number of applications for DLMs have been developed which depend on the selection of materials in each layer [41]. These applications include gas separation [42], ultrafiltration [43], nano-filtration [44], organic solvent nano-filtration [45], forward osmosis and pressure retarded osmosis [46], membrane distillation [47], pervaporation [48] and photocatalytic degradation [49].

In this study, a novel DL bicomponent functional NFM of PAN-NFs as a supporter and PA/Ch-NFs as a top hydrophilic coating layer was fabricated. The efficiency of the prepared DLNFM for capturing dye residues and heavy metals from wastewater was examined.

2. Materials and methods

2.1. Materials

PA waste fibers with an average molar mass of 22500 g/mol were collected from Misr Beida Dyers Company, Egypt. PAN waste fibers were obtained by the Egyptian Company for Manufacturing Acrylic Yarns. Formic acid (98 %) and dimethylformamide (DMF) were purchased from Fisher Chemical Company. Ch with molecular weight 100000: 300000 was supplied from Sigma Aldrich. Reactive red dye 24 and C.I acid blue 203 was supplied by Egypt Synthetic Colors Company, Cairo, Egypt. All other chemicals are of laboratory grade used without further purification.

Table (1) indicates the all samples of the article.

2.2. Methods

2.2.1. Preparation of electro-spun solution

8 % (w/v) solution of PAN was prepared by dissolving PAN fibers in DMF at 60 °C under shaking overnight to obtain an electro-spinnable clear solution. A 15 % (w/v) solution of PA was prepared by dissolving PA fibers in formic acid at room temperature using a magnetic stirrer for 1h.

Based on several preliminary trials to attain electro-spinnable composite solutions, the composite of PA/Ch was prepared by using different ratios of Ch (0.25, 0.5, 0.75, 1, and 1.25 %) to 15 % PA where Ch was firstly added little by little to formic acid with continuous stirring using a magnetic stirrer at 500 rpm speed and left overnight at room temperature to obtain a clear viscous solution after that PA was added to the chitosan solution until complete dissolution.

2.2.2. Preparation of the nano-fibrous mat

The prepared PAN, PA, as well as PA/Ch composite solutions were, electro-spuned into NFM using ELMARCO nozzle-less Electro-spinneret (Liberec, Czech Republic), using electric potential 25–30 kV. The solution carriage speed was set at 100 mm/s, which was determined to be the ideal speed for the production of NFs, and the collector, was located 13.5 cm from the wire. The electro-spinning process was carried out at 25 °C and 51 % relative humidity.

2.2.3. Preparation of dual-layer membrane

10 ml of PAN solution was electro-spun to obtain the first layer of DLM under the aforementioned condition of the electro-spinning. After that 30 ml of the prepared PA/Ch composite solution was electro-spun above the PAN NF layer. The obtained bi-layer NFM was then dried in an oven at 60 °C for 2 h to ensure complete evaporation of the used solvents and then pressed using a hot press at 140 °C with a pressure of 10 kg/cm2 for 10 s.

2.2.4. Preparation of heavy metal and dye solutions

For this investigation, three stock solutions of 20 ppm/L of chromium III chloride hexahydrate [CrCl3.6H2O], lead acetate [(CH3COO) 2 Pb], and copper II sulfate pentahydrate [CuSO4.5H2O] were prepared as synthetic wastewater. The pH of the prepared stock solutions was not modified and used as it is at 6.5.

For preparation dye solution, 1 g/L solutions of Reactive Red 24 and Acid Blue 203 dyes were prepared by adjusting the pH of the prepared dye solution at 5 for Reactive dye and 4.5 for Acid dye.

2.3. Analyses and testing

2.3.1. Viscosity measurement

The viscosity of the prepared composite solutions was measured by using a Brookfield vZiscometer (DV-E Brookfield Engineering Labs Inc., Middleboro, MA, USA) at 100 rpm.

2.3.2. Scanning electron microscopy

The produced NFMs' surface morphology and fiber diameter were studied using a ZEISS LEO 1530 Gemini Optics Lens Scanning Electron Microscope (SEM) with a scanning voltage of 30 kV. The samples were put on aluminum stubs and covered with gold using an S150A sputter (coated Edward, UK). Scanning electron micrographs of the NFs were used to estimate their diameters and porosity.

2.3.3. Fourier transform infrared spectroscopy (FT-IR)

2.3.4. FT-IR analysis was conducted on the produced NFMs using JASCO FTIR-4700 from Japan. The analysis was performed in a range of 4000-400 cm^{-1} with a spectral resolution of 4.0 cm^{-1}.

2.3.4. Thermal properties

SDT Q2000 Tzero DSC from TA tools was used to measure thermal gravimetric analyses (TGA) and differential scanning calorimetry (DSC) of NFMs under a nitrogen atmosphere with a heating rate of 10 °C/min.

2.3.5. X-ray diffraction (XRD) pattern

On a Bruker D8 Avance with Cu K as the target and a secondary monochromator set to 40 KV and 40 mA, the XRD pattern of the obtained NFM has been evaluated. In reflection geometry, the scans were carried out with a scanning step of 0.02° and within a range of $4° < 2\theta < 60°$. The following empirical equation, labeled as Eq. (1), was utilized to calculate the crystallinity index (CI).

$$CI = [(Ic - Ia) / Ic]x\ 100 \quad \text{Eq.(1)}$$

Where Ic is the highest intensity of crystal lattice diffraction, Ia is the minimum intensity, and CI is the crystallinity index. Higher CI values often suggest that the NF sample is more crystalline.

2.3.6. Air permeability

An FX 3300 air permeability tester (TEXTEST AG, Switzerland) at the pressure of 100 Pa was used to evaluate the produced mats' air permeability according to ASTM D737 standard method [50].

2.3.7. Water permeability

The water permeability of the obtained NFM was evaluated according to the ASTM-D 1913 (American Test Method for Water Repellency; Water Spray Test new edition 2010).

2.3.8. Dye adsorption

0.01 g of the prepared NFM was submerged in 10 mL of the prepared reactive dye and acid dye at room temperature. Dye adsorption by NFMs was detected spectrophotometrically after different intervals (2, 24, 48, 72, and 96 h) at λ_{max} 485 nm for reactive dye and λ_{max} 575 nm for acid dye. In another study, dye adsorption by NFMs was detected after 1hr at 60 °C. Dye removal percent (dye adsorption %) was calculated according to Eq. (2)

$$\text{Dye adsorption } \% = \frac{A_{\text{ before}} - A_{\text{ after}}}{A \text{ before}} \text{ X } 100 \qquad \text{Eq.(2)}$$

Where "A **before**" is absorbance of the prepared dye, and "A **after**" is absorbance of dye bath after contacting with NFMs after several intervals.

2.3.9. Batch sorption investigation

By using a batch approach and a single-element system across various contact durations, the chelating ability of NFMs to bind Cu^{+2}, Cr^{+3}, and Pb^{+2} cations was observed. A dried sample weighing 0.025 gm of each produced mat was immersed in an Erlenmeyer flask that already contained 25 mL of each cation solution. For the 2, 10, 24, 48, 72, and 96-hr periods, the mixture was kept at 25 °C with minimal stirring. An atomic absorption spectrometer, the PerkinElmer Analyst 4100 ZL [51], was used to filter the solution and detect the metal ion concentration.

The removal efficiency percent of heavy metal by NFMs was calculated according to the following Eq. (3)

$$\text{Removal efficiency } \% = \frac{C_{\text{ before}} - C_{\text{ after}}}{C \text{ before}} \text{ X } 100 \qquad \text{Eq.(3)}$$

While "C **before**" is the concentration of metal cation in stock solution and "C **after**" is the concentration of metal cation after contact by NFMs after different periods.

3. 3results and discussion

Despite the NFM having a considerable application for wastewater purification; its bad mechanical properties and abrasion resistance under loading are still some of its disadvantages. Several techniques have been developed to get rid of the mechanical fragility of NFMs. Those approaches include fiber orientation and alignment [52], fiber blending [53], reinforcement [54], additives [55], epoxy composite [56], carbonization [57], inter-fiber bonding by using chemical crosslinking or heat treatment [58], ultrasonic welding [59], dip-coating [60], thermal lamination and heat press [61]. Industrially, the thermal lamination and heat press processes are more promising for membrane production while the other approaches are not eco-friendly, time waste, costly, and some are not effective for long-term application [62].

Table 1
Weight and percent of each polymer of the sample weight.

#	Sample	gm_s			%		
		PAN	**PA**	**Ch**	**PAN**	**PA**	**Ch**
1	PAN-NFs	3.2	–	–	100	–	–
2	PA-NFs	–	6	–	–	100	–
3	PA/0.25%Ch-NFs	–	5.9	0.1	–	98.3	1.7
4	PA/0.5%Ch-NFs	–	5.8	0.2	–	96.7	3.3
5	PA/0.75%Ch-NFs	–	5.7	0.3	–	95	5
6	PA/1%Ch-NFs	–	5.6	0.4	–	93.3	6.7
7	PA/1.25%Ch-NFs	–	5.5	0.5	–	91.7	8.3
8	DL(PAN/PA-0.25%Ch) NFs	0.8	4.425	0.075	25	73.75	1.25
9	DL(PAN/PA-0.5%Ch) NFs	0.8	4.35	0.15	25	72.5	2.5
10	DL(PAN/PA-0.75%Ch) NFs	0.8	4.275	0.225	25	71.25	3.75
11	DL(PAN/PA-1%Ch) NFs	0.8	4.2	0.3	25	70	5
12	DL(PAN/PA-1.25%Ch) NFs	0.8	4.125	0.375	25	68.75	6.25

3.1. Viscosity of the prepared electro-spun solutions

The viscoelastic properties of the polymer solution are considered an important key parameter of the electro-spinning process [63]. These characteristics were adjusted by monitoring the polymer concentration which controls the electro-spinnability of fiber as well as its influence on the obtained fiber morphology and diameter [64] (see Table 1).

Results of Table 2 show that the viscosity of PA solution is higher than PAN due to the higher concentration of PA (15 %) compared to that of PAN (8 %). The electro-spun solution should have enough concentration of polymer for chain tangles occurrence; however, the solution cannot be either too concentrated or too dilute. The concentration of polymer affects both the viscosity and the surface tension of the solution, where both of which are significant parameters in the electro-spinning process [65]. As can be seen in Table 2, by increasing the concentration of Ch, the viscosity of the obtained PA composite solutions increased which influenced the obtained NFs diameter as well as the fibers ' pore size.

3.2. Characterization of nano-fibrous

3.2.1. Nano-fiber morphology and properties

Figures (1-3) display SEM images of NFMs obtained by electro-spinning of PAN, PA, and PA composites with different concentrations of Ch as well as un-pressed and pressed DL PAN/PA and PAN/PA-Ch. The micrograph images display a random distribution and interconnected structure of micro- and NFs with no beads formed, giving a non-woven web. These obtained NFMs exhibit a large surface area that would effectively capture heavy metals and dyes from industrial effluent. These NFs have several diameters based on the prepared polymer solution viscosity. Both experimental and theoretical studies have shown that NF diameter strongly affects the pore size whereby the pore size increases by increasing the fiber diameter [66].

As shown in Fig. 1 and Table 3, the PA solution produced a large fiber diameter with a large pore size compared with the PAN solution. This is due to not only the higher viscosity of PA solution than PAN but also the volatility of the applied solvent. where the volatility of formic acid that used in the dissolution of PA is higher than that of DMF used in PAN dissolution [67]. Moreover, as solvent volatility increased the pore size increased. This is due to more volatile solvents evaporating faster leading to increasing polymer concentration and viscosity during the electro-spinning process resulting in larger fiber diameter and pore size [67].

On the contrary, as observed in Fig. 2 and Table 3 the diameter of electro-spun NFs was decreased when Ch concentration increased. This finding is due to Ch being a cationic polysaccharide, with amino groups at the C_2 position which are ionizable under acidic or neutral pH conditions. During electro-spinning, this polymer causes a higher charge density to form on the surface of the ejected jet. As the charges carried by the jet increase, higher elongation forces are imposed on the jet under the applied electrical field. This indicates that the repulsive forces between ionic groups in the Ch backbone blocked the formation of continuous fiber during electro-spinning [68].

Pores of NFMs are caused by the entanglement of the NFs, as more NFs covering a specific area would result in narrower pore size distribution along with smaller pores that are observed for DLNFMs [69]. It has been mentioned that fine fibers of low diameters give small pore sizes with high density and filtration efficiency to filter media [70].

On another hand, a rapid hot-pressing of the membrane that was performed for a few seconds helped to fuse the fibers forming a stable dimensional network of electro-spun fibers with a reduced thickness which assisted in improving the mechanical properties of the obtained membrane [71].

As seen in Fig. 3, after hot pressing, fibers of the two layers are diffused together and cannot be differentiated from each other. Additionally, data from Table 3 show that, the mean pore size of hot-pressed PAN/PA, PAN/PA- 0.75%Ch, and PAN/PA- 1.25%Ch-NFs shifts to 0.158, 0.074, and 0.067 mm compared with un-pressed DLMs 0.35, 0.167 and 0.16 mm; respectively. This may be explained in terms of the hot press can transport the fibers closer together resulting in smaller pores and a smoother surface by the formation of a much more regular structure [47].

3.2.2. Thermal properties

TGA and DSC were used to monitor the thermal behavior of the prepared NFM, as shown in Figures (4-8).

Fig. 4 clarifies that the maximum weight loss of PAN-NFs is 30 % at 616.7 °C. The thermogram of PA-NFs shows a weight loss of 80 % in the range (391.5–429 °C) owing to the loss of water and low molecular weight compounds [72]. The maximum weight loss of the electro-spun PA-NFs is 80 % at 429 °C which may be due to the degradation of PA. As shown in Fig. 5, the thermogram of PA/Ch (0.75,

Table 2
Viscosity of the PAN, PA and different concentrations of PA/Ch composite solutions.

Sample	Viscosity(cp)
PAN	2.2
PA	4
PA/0.25%Ch	5.4
PA/0.5%Ch	8.6
PA/0.75%Ch	11.8
PA/1%Ch	19.8
PA/1.25%Ch	22.2

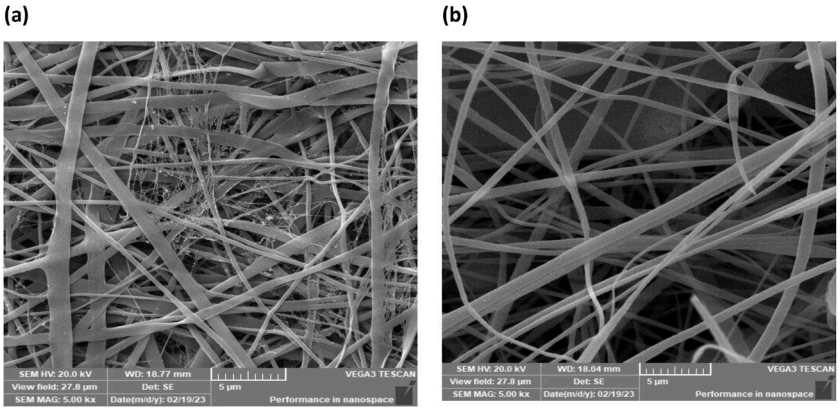

Fig. 1. Sem of (a) PA-NFs and (b) PAN-NFs.

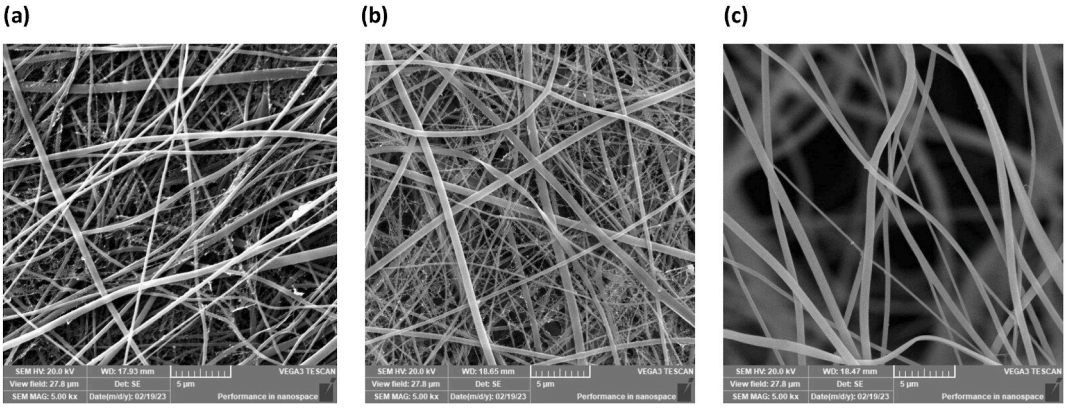

Fig. 2. Sem of (a) PA/0.25%Ch-NFs, (b) PA/0.75%Ch-NFs, and (c) PA/1.25%Ch-NFs.

1.25 %) NFMs displays low weight loss of (48 % and 35.4 %) in the range starting from 408 to 496 °C and 416–501 °C, respectively. This is due to the decomposition of Ch, i.e. dehydration of the saccharide rings, depolymerization, and decomposition of the acetylated and deacetylated units of the Ch. It has been mentioned that Ch-NFs started to decompose at temperatures above 200 °C [73]. Moreover, the maximum weight loss of PA/0.75%Ch and PA/1.25%Ch NFMs are 48 % and 35.4 % at 496 °C and 501 °C, respectively. These results confirmed the high thermal stability of PA-NFM in the presence of Ch with various concentrations.

In the case of the DLMs, as presented in Fig. 6, it is observed that the maximum weight loss of the un-pressed and pressed NFMs reached 44.7 % and 52.3 % at 616.8 °C and 617 °C, respectively. This increase in the thermal stability of the bi-layered NFMs was attributed to the entanglement of the two polymer molecular chains and so limiting the thermal motion [74]. Furthermore, the decomposition temperature of the Ch functionalized DLMs reached about 617 °C with a maximum weight loss of 60 %, see Figs. 7 and 8. This is due to the presence of chitosan polymer resulting in strengthening the produced bi-layered membrane to get the highest thermal stability compared with the other NFMs.

DSC thermograms of all PA-NFMs show endothermic peaks in the range of 200–440 °C while PAN is exothermic in the range of 100–410 °C. The electro-spun PA-NFs exhibited a glass transition temperature in the range of 210–261 °C [75]. As observed in Fig. 5 (b), the electro-spun PA/Ch-NFs exhibited a systematic reduction in the glass transition temperature (Tg) from 220.77 °C of pure PA-NF to 217.191 °C and 216.59 °C of PA/0.75%Ch and PA/1.25%Ch respectively. This may be due to changes in the crystalline phase with increasing Ch contents thereby reducing the transition temperature of the polymer [75]. Furthermore, melting temperature (T_m) increased from 402.978 °C for PA-NFs to 433.271 and 435.541 °C for PA/Ch-NFs which indicates the enforcement of the NFs by the addition of chitosan resulting in improving the thermal stability of the PA/Ch-NFMs.

PAN is a semicrystalline polymer in which the Tg value primarily depends on the amorphous part of the PAN structure [76]. Fig. 4 (b) shows that the Tg of PAN-NFM is 109.369 °C and T_m is an exothermic peak at 312.745 °C. This can be attributed to the cyclization of PAN molecular chains which is a highly exothermic process and is accompanied by the growth of a large amount of heat that can promote cyclization of the nitrile group in PAN [77].

DSC thermograms of DLNFMs show the presence of both endo and exothermic peaks of PA and PAN-NFs with slight shifting that proves these bi-layered NFs are physically bonded and the hot-press step dose not strictly influence the thermal stability of these DLMs.

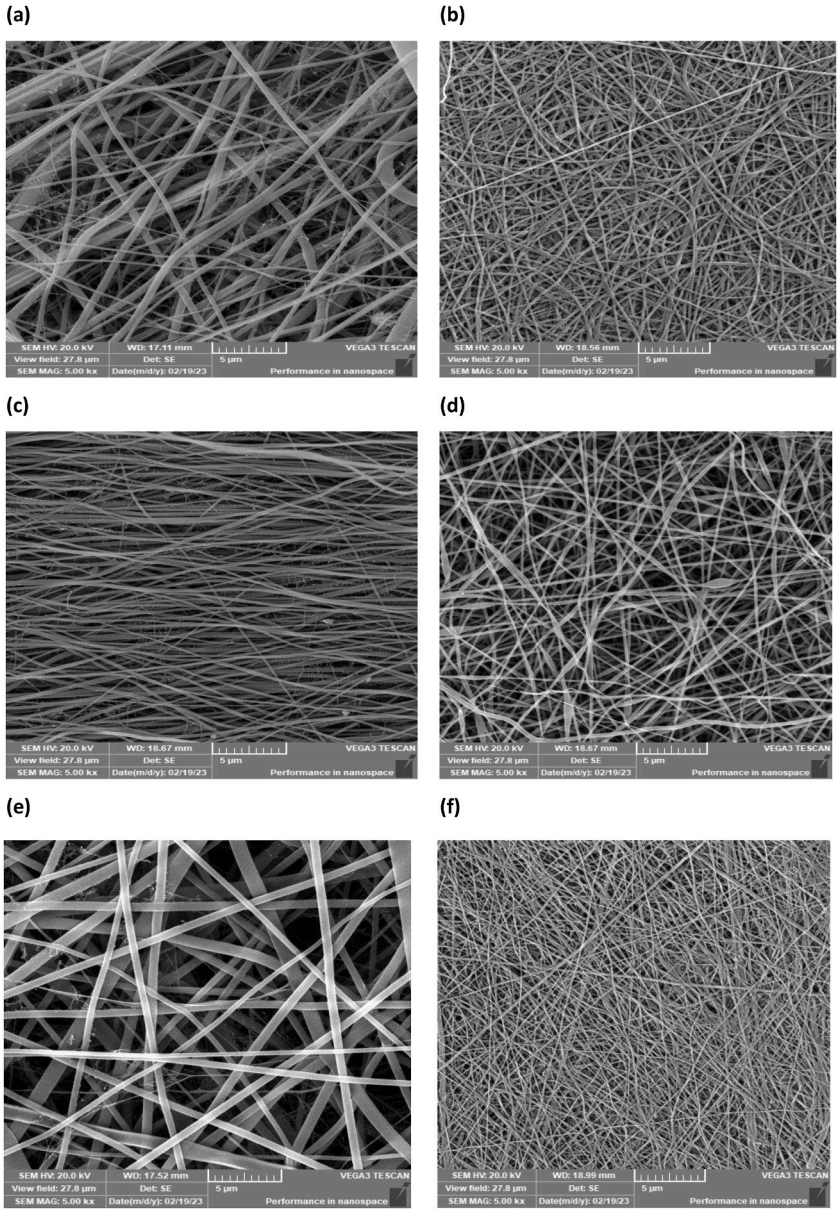

Fig. 3. SEM of (a) un-pressed and (b) pressed DL PAN/PA-NFs, (c) un-pressed and (d) pressed DL PAN/PA-0.75%Ch-NFs, (e) un-pressed and (f) pressed DL PAN/PA-1.25%Ch-NFs.

3.2.3. Fourier transform infrared spectroscopy

FT-IR spectroscopy was applied to study the chemical changes that occur by blending Ch with PA as well as any alternation in DLNFMs. Fig. 9(a–e) shows the FT-IR spectra of the PA, PA/0.75%Ch, PA/1.25%Ch, and PAN, as well as un-pressed and pressed DLNFMs. Fig. 9(a) explains the interaction between the PA and Ch. Generally, there is no noteworthy difference between PA and PA/Ch-NFs peaks. As shown in Fig. 9(a) it can be observed a band in the region of about 3300 cm^{-1} corresponded to the amide (N–H stretching) and 3085 cm^{-1} referred to the overtone of N–H bending. The transmittance band at 2931 cm^{-1} and 2859 cm^{-1} is indicated to be symmetric and asymmetric CH_2 stretching vibration, respectively [78]. There are intense double absorption bands at 1630 and 1550 cm^{-1} which are related to C═O stretching and in-plane N–H bend of amide groups [79]. The band at about 1370 cm^{-1} was assigned to the symmetrical deformation of CH_3 in the amide group [80]. Furthermore, bands at about 1270 cm^{-1} are assigned to C–N stretching and a peak at 690 cm^{-1} is specialized for out-of-plane N–H bending [81]. However, as can be seen, the intensity of all the as-mentioned characteristic bands was found to be decreased with increasing Ch concentration in PA/Ch blended NFs and this may be due to the formation of hydrogen bonding between Ch and PA [82].

As shown in Fig. 9(b) the FT-IR spectra of PAN-NFs displayed the stretching vibrations of –OH bond that appeared between 3600

Table 3
Fiber diameter and pore size of the obtained electro-spun NFs from different polymeric solutions.

Sample	Mean fiber diameter (nm[(a)])	Mean pore size (nm)
PAN-NFs	500	1900
PA-NFs	370	4600
PA/0.25%Ch-NFs	240	190
PA/0.75%Ch-NFs	240	290
PA/1.25%Ch-NFs	300	280
Un-pressed DL (PAN/PA) NFs	160	220
Pressed DL (PAN/PA) NFs	150	100
Un-pressed DL (PAN/PA-0.75%Ch) NFs	140	300
Pressed DL (PAN/PA-0.75%Ch) NFs	90	66
Un-pressed DL (PAN/PA-1.25%Ch) NFs	300	360
Pressed DL (PAN/PA-1.25%Ch) NFs	120	240

(a) Average diameter of 11 measurements of 11 different NFs.

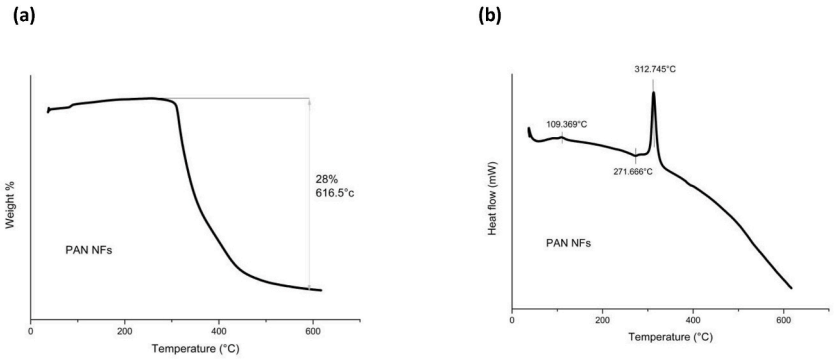

Fig. 4. TGA (a) and DSC (b) curves of PAN-NFs.

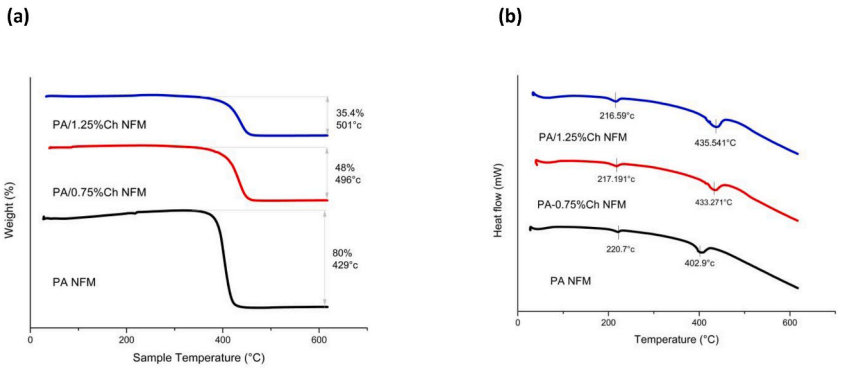

Fig. 5. TGA (a) and DSC (b) curves of PA, PA/0.75%Ch and PA/1.25%Ch-NFM.

and 3500 cm^{-1} from the absorbed water. The band appeared at 2936 cm^{-1} is related to aliphatic C–H vibrations. The intensity at 2240 cm^{-1} corresponds to the nitrile (–C≡N) group at around [83]. The intensities at 1730 and 1620 cm^{-1} are due to C═O in the carbonyl group and C═C vibrations respectively. Furthermore, the two bands located at 1450 cm^{-1} for C–H tensile vibration in the CH_2 group and 1360 cm^{-1} for C–H stretching which are characteristics of aliphatic CH groups along the PAN backbone [84]. The band at 1240 cm^{-1} is assigned to C–O vibrations while the signal at 1050 cm^{-1} and 995 cm^{-1} is attributed to C–N bonds [85]. Additionally, the two absorption bands around 640 cm^{-1} and 780 cm^{-1} were referred to as the stretching vibrations of = CH and N–H, respectively.

FT-IR spectra of the DL show the characteristic bands of both PA-1.25%Ch and PAN and their position in bi-layered PA-1.25%Ch/PAN-NFs (un-pressed and pressed) appeare without change. This indicates that the chemical composition of both PA-1.25%Ch and PAN remains the same even after hot-press. This also proves that the degree of cross-linking is at a very minimum level whereby it helps both PA-1.25%Ch and PAN to be physically attached without affecting their respective chemical compositions.

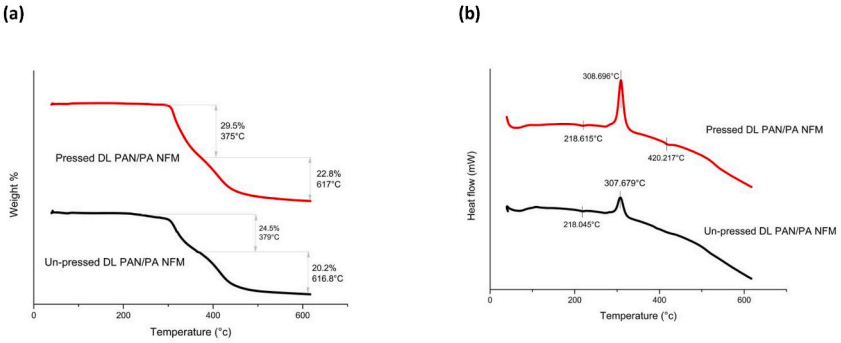

Fig. 6. TGA (a) and DSC (b) curves of un-pressed and pressed DL (PAN/PA) NFM.

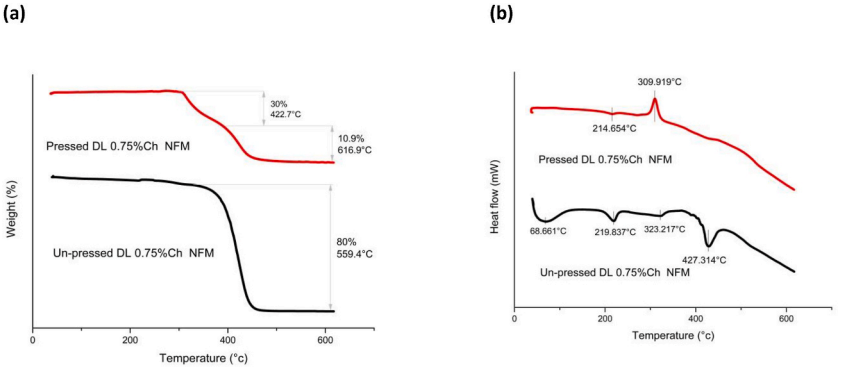

Fig. 7. TGA (a) and DSC (b) curves of un-pressed and pressed DL (PA, PA/0.75%Ch) NFMs.

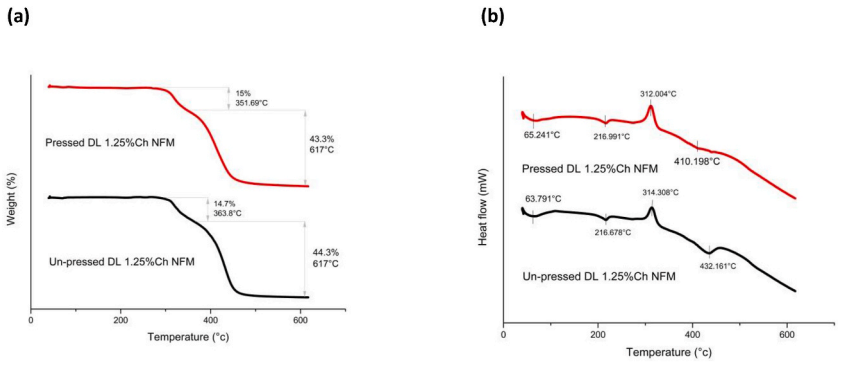

Fig. 8. TGA (a) and DSC (b) curves of un-pressed and pressed DL (PA, PA/1.25%Ch) NFMs.

3.2.4. X-ray diffraction pattern

The crystal phase and structure of the prepared electro-spun NFMs were identified by XRD. As appeared in Fig. 10(a), PAN-NFs exhibit intense peaks at $2\theta = 16.6^{\circ}$ and a small one at 28.8°. From Fig. 10(b), the XRD pattern of PA-NFs displayed a wide peak that appeared at $2\theta \simeq 20^{\circ}$ with a d-spacing of 4.5 which is associated with the crystal plane of PA to rapid evaporation of solvent (formic acid) during the electro-spinning process [86]. By blending PA with Ch, the 2θ peaks are shifted gradually toward a higher field by the addition of Ch, which means that the d-spacings between the plane are decreased indicating the interaction between Ch and PA [87]. XRD pattern of the prepared PA/Ch-NF is formed by their characteristic two peaks between 20 and 25° [88]. As appeared in Fig. 10(c) and Table 4, the characteristic peaks of both PAN and PA appeared in un-pressed and pressed PAN/PA-DLNFs.

Table 4 declared that the crystallinity of PA-0.75%Ch and PA-1.25%Ch-NFs is greater than that of the PA-NFs. This could be explained by the formation of physical interactions, (hydrogen bonds), between PA and Ch which reduce the freedom of the polymer chains leading to the development of further crystalline areas [88]. Furthermore, increasing the concentration of Ch results in more reinforcement of the obtained NFM, leading to more crystallinity percent.

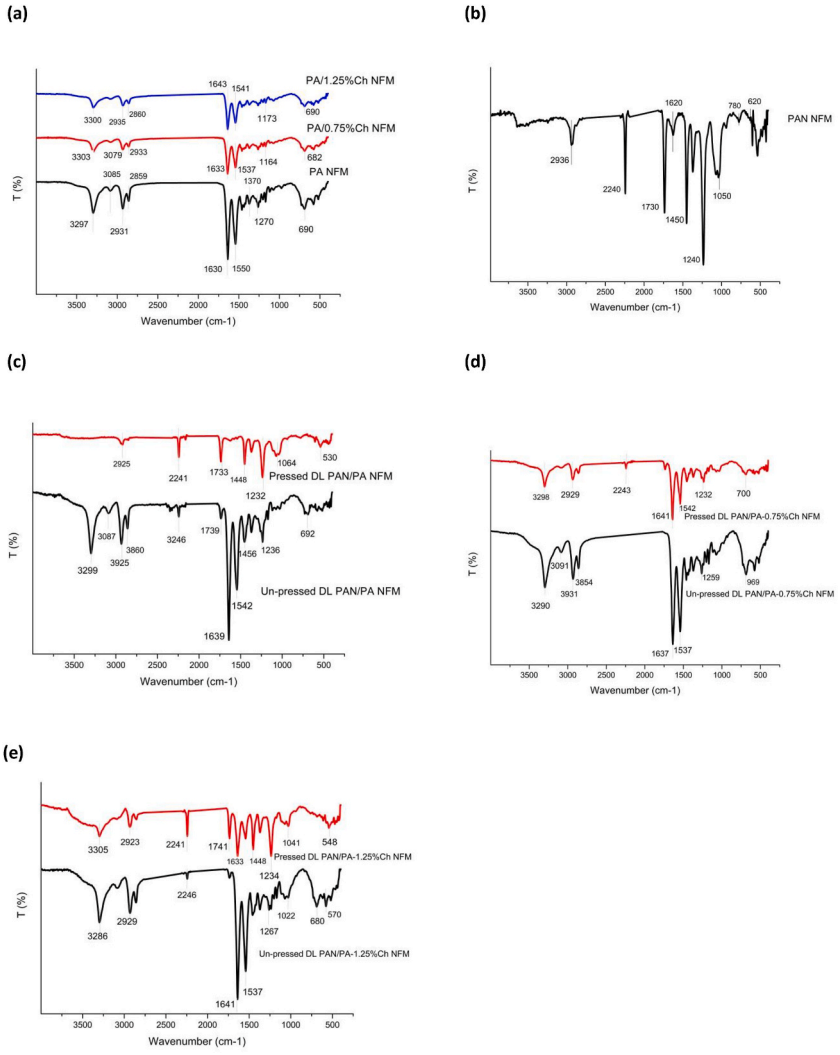

Fig. 9. FTIR charts of (a) PA, PA/0.75%Ch, PA/1.25%Ch, (b) PAN, (c) pressed and un-pressed DL PAN/PA, (d) pressed and un-pressed DL PAN/PA-0.75%Ch and (e) pressed and un-pressed DL PAN/PA-1.25%Ch NFMs.

On another hand, data from Table 4 reveals that there is a noticeable change in the crystallinity of nano-fiber before and after hot-pressing, indicating that the fiber membrane melt changes under hot-pressing. It has been pointed out, that under hot temperatures the recrystallization of the polymer NFs occurred causing the formation of α crystalline structure resulting in an acceptable decrease in crystallinity of the polymeric fiber [89].

3.2.5. Air and water permeability

Air and water permeability are vital to NFM applications among which is membrane distillation. Different parameters can affect the air and water permeability of NFMs including fiber diameter, membrane thickness, and porosity [90]. Due to the weakness of the mechanical properties of single-layer NFM, its application in the water filtration area is limited. As a result of this problem, NFM requires an additional supporting layer with hot press to provide strength [91].

As clear in Table 5, the thickness of the obtained hot-pressed NFMs is lower than the un-pressed ones. This may be due to the hot-press process causing the fibers to be close together resulting in a thin membrane. Furthermore, by increasing the concentration of Ch in the composite solution, the thickness of the obtained mat decreased due to the gradual decrease in the diameter of the obtained NFs.

Data from Table 5 also shows decreasing in air permeability after the hot-press process. This can be explained in terms of during the heat press process the NFMs' porous structure and void space can be decreased due to the overlapping of NFs under compression. It has been reported that by reduction the porosity and open pore structure of NFM air permeability is decreased [92].

Furthermore, the changes in the water permeability of the membrane are also related to pore structure, pores interconnection, thickness of membrane, and affinity to water absorption [93]. Results of Table 5 show the influence of the affinity of the membrane to water absorption as well as its thickness on water permeability. It is observed that as the membrane thickness decreased, water

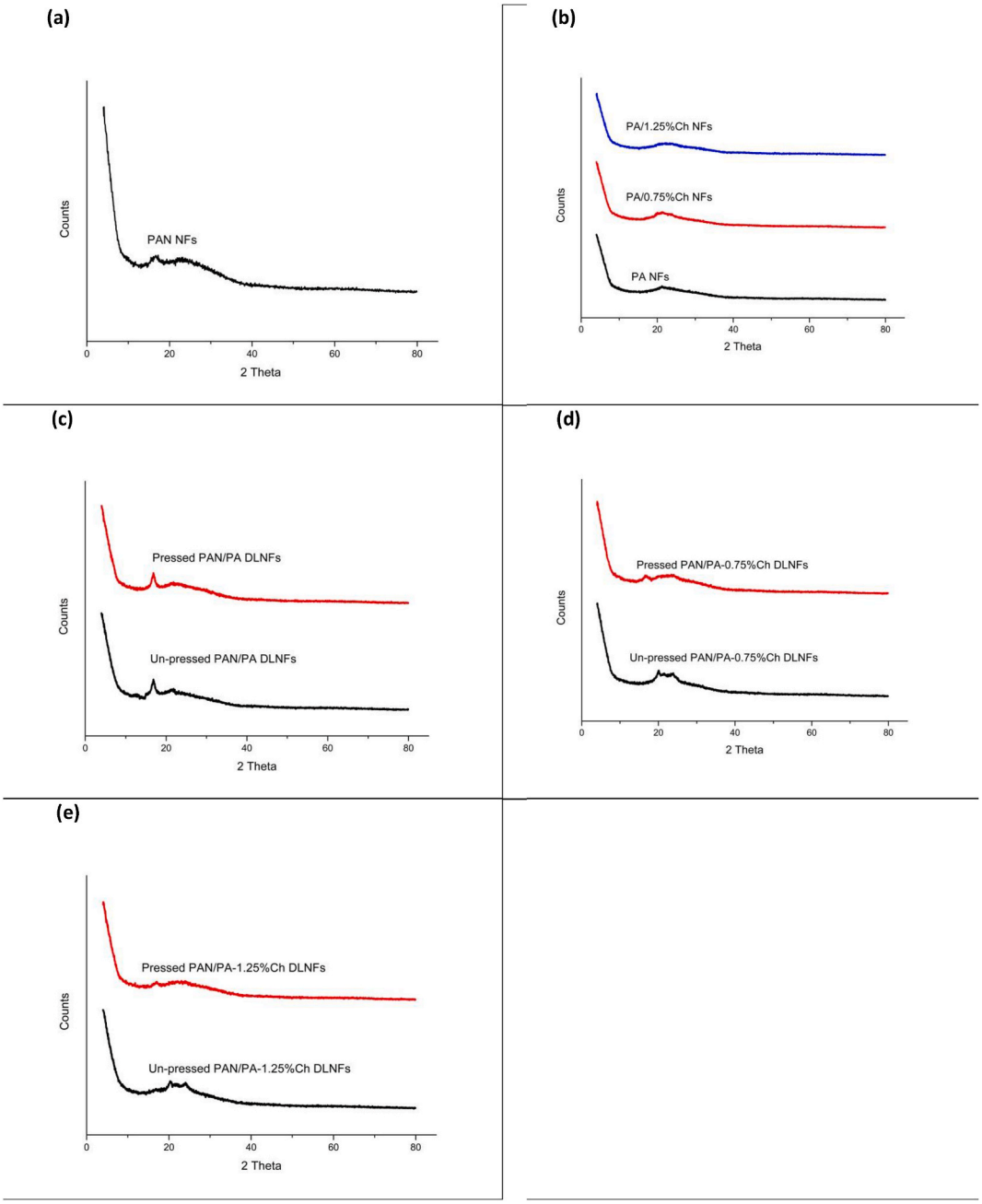

Fig. 10. XRD pattern of: (a) PAN-NFs, (b) PA-NFs, PA-0.75%Ch-NFs, PA-1.25%Ch-NFs, (c) un-pressed and pressed PAN/PA-DLNFs, (d) un-pressed and pressed PAN/PA6-0.75%Ch DLNFs, and (e) un-pressed and pressed PAN/PA-1.25%Ch-DLNFs.

permeability increased.

3.3. Application of the prepared membranes in water purification

The filtration process occurs by various mechanisms depending on the size or charge of the particles to be filtered. Gravity sedimentation and inertial impact ion mechanisms occur for the retention of larger particles, interception diffusion for blocking small particles, and electrostatic attraction. Electrostatic attraction happens in particles of different dimensions and takes place when the fibers are electrically charged which attracts the oppositely charged particles [94]. NFMs have higher filtration efficiencies due to their controllable small diameter, low basis weight with reduced thickness, and porous structure as well as high permeability values [93].

Table 4
Crystal structure of (a) PA-NFs, PAN-NFs, PA-0.75 % Ch-NFs, (b) PA-1.25%Ch-NFs, (c) un-pressed and pressed PAN/PA-DLNFs, (d) un-pressed and pressed PAN/PA-0.75%Ch-DLNFs, (e) un-pressed and pressed PAN/PA-1.25%Ch-DLNFs.

Sample	2 Θ	d-spacing Å	Crystallinity index (%)
PA-NFs	19.3	4.5	13.8
PAN-NFs	16.6	5.3	10.6
	28.8	5.1	
PA-0.75%Ch-NFs	20.1	4.1	15.1
	24.5	4.3	
PA-1.25%Ch-NFs	21.4	4.1	21.1
	23.8	3.7	
Un-pressed DL PAN/PA-NFs	12.8	6.8	18.9
	19.8	4.4	
Pressed DL PAN/PA-NFs	16.8	5.2	14.9
	31.6	2.8	
Un-pressed DL PAN/PA-0.75%Ch-NFs	20	4.4	18.4
	23.7	3.7	
	24.6	3.6	
	31.5	2.8	
	37.7	2.8	
Pressed DL PAN/PA-0.75%Ch-NFs	16.8	5.2	12.8
	20	4.4	
Un-pressed DL PAN/PA-1.25%Ch-NFs	20.2	4.3	29.6
	24	3.7	
Pressed DL PAN/PA-1.25%Ch-NFs	16.9	5.2	24

Table 5
Thickness, air and water permeability of the prepared DL NFMs.

Sample	Thickness (mm)	Air permeability ($Cm^3/Cm^2.S$)	Water permeability (L/Sec.), Δh = 100 mm
Un-pressed DL (PAN/PA) NFM	0.3	5.72	462.6
Un-pressed DL (PAN/PA-0.25%Ch) NFM	0.28	5.31	480.8
Un-pressed DL (PAN/PA-0.5%Ch) NFM	0.28	5.44	495
Un-pressed DL (PAN/PA-0.75%Ch) NFM	0.26	5.68	520.9
Un-pressed DL (PAN/PA-1%Ch) NFM	0.2	5.72	610
Un-pressed DL (PAN/PA-1.25%Ch) NFM	0.17	5.88	655.1
pressed DL (PAN/PA) NFM	0.16	3.61	687.4
pressed DL (PAN/PA-0.25%Ch) NFM	0.15	3.59	722.5
Pressed DL (PAN/PA-0.5%Ch) NFM	0.13	3.51	780
pressed DL (PAN/PA-0.75%Ch) NFM	0.11	3.35	830.8
pressed DL (PAN/PA-1%Ch) NFM	0.09	3.03	861.2
pressed DL (PAN/PA-1.25%Ch) NFM	0.08	3.01	956.9

3.3.1. Dye adsorption

Wastewater effluent from textile industrial processes is polluted by various dyes, which are carcinogenic, non-biodegradable, and contaminating fresh water. On the other hand, the typical treatment methods are not efficient enough due to technical and economic reasons. So, different techniques have been developed for the dye removal [2]. Membranes are the main of great interest for effluent treatment where the systems do not need any addition of chemical agents [3].

Several natural biopolymers have been successfully electro-spun producing functional nano-fibers membranes which displayed a unique capability for water purification by filtration [2]. chitosan, as a natural bio-polymer, has remarkable absorption capabilities alongside it has high contents of amino and hydroxyl functional groups [95]. Due to these properties, chitosan is broadly applied in the removal of pollution from wastewater [96]. Consequently, the assistance of the biopolymer is taken from combining both chitosan and PA and converting them into NFs by using the electro-spinning method [88].

Figures (11, and 13) show the efficiency of the prepared NFMs of PAN, PA as well as PA with different concentrations of Ch toward the adsorption of anionic dyes (acid and reactive dyes) after contacting for several intervals at room temperature and after an hour at 60 °C. It is observed that there is no affinity of PAN-NFs toward the adsorption of both types of anionic dyes compared with PA-NFs. This may be due to PAN has no functional group to adsorb anionic dyes. There is electrostatic attraction between positively charged amino groups of PA-NFs and dye anions at acidic pH. On the other hand, the presence of Ch in PA-NFs greatly increases dye adsorption reaching up to 90 %. this is because at acidic pH the amino groups of Ch are protonated leading to strong electrostatic interaction between the membrane surface and the dye anions which results in more increase in dye adsorption [95].

As indicated in Fig. 11, the removal efficiency increased by increasing both the Ch ratio and contact time. The maximum removal efficiency of acid dyes reached to 97 % and of reactive dye was approximately 73%for PA-1.25%Ch after 3 days at room temperature.

As more clarify, Fig. 12 shows the capacity of PA/1.25%Ch-NFs toward adsorption of acid dye at room temperature after 3 days compared with that of PA-NFs.

Additionally, as seen in Fig. 13, by increasing the temperature of the dye bath (60 °C) the capacity of dye removal rapidly increased

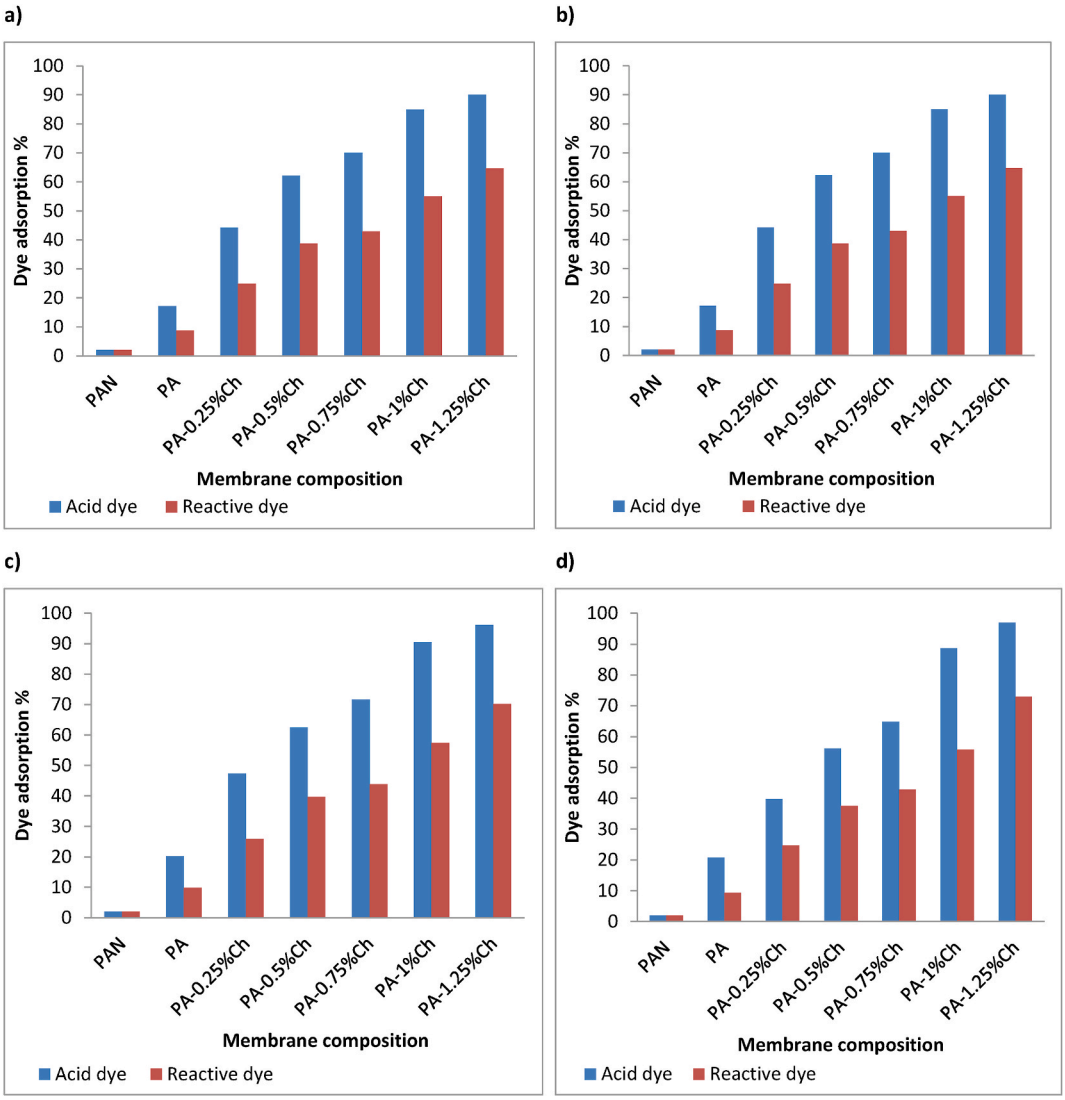

Fig. 11. Adsorption of anionic dyes (acid and reactive) by PAN, PA and PA/Ch-NFMs at room temperature after a) 1hr, b) 1day, c) 2 days and d) 3 days.

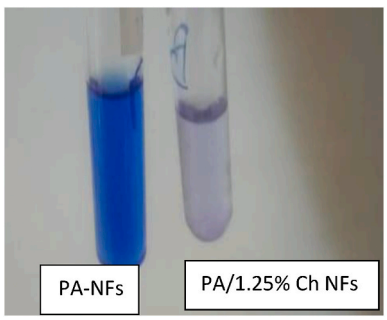

Fig. 12. Adsorption capacity of acid dye by PA and PA-1.25%Ch-NFs after 3 days at room temperature.

reaching about 88 % for acid dye and 53 % for reactive dye after only an hour.

Fig. 14(a–d) explains the capacity of the prepared DLNFs containing different amounts of Ch toward adsorption of anionic dyes for several periods at room temperature. Generally, the dye adsorption by the DLNFs increased by either increasing the concentration of

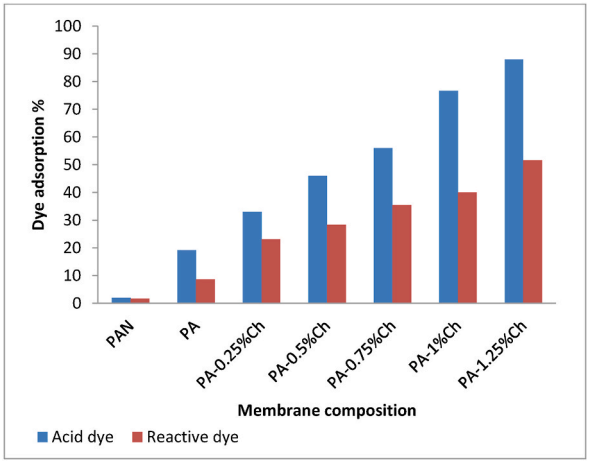

Fig. 13. Adsorption of anionic dyes (acid and reactive) by PAN, PA and PA/Ch-NFMs at 60 °C for 1hr a).

Ch as well as contact time.

On the other hand, the efficiency of the DLNFs toward the dye adsorption is relatively lower than that of PA/Ch-NFs. this may be due to the presence of the PAN-NFs supporter layer, in DLNFs which does not affect the adsorption of the dye. The maximum removal efficiency of acid dyes reached about 73.4 %, and of reactive dye was approximately 61 % for PAN/PA-1.25%Ch DL after 3 days at room temperature (see Fig. 15).

Furthermore, by studying the effect of temperature on the adsorption capacity of the dye by DLNFs, it is observed the dye removal rapidly increased which attained about 70 % for acid dye and 51 % for reactive dye after only 1 h at 60 °C by PAN/PA-1.25%Ch DLNFs. Fig. 16(a–d) are more clarify the anionic dye adsorption capacity of PAN/PA-1.25%Ch-DLNFs after 3 days at room temperature as well as after 1 h at 60 °C.

3.3.2. Metal adsorption

Pollution of discharged water from several manufacturers such as textile, dye manufacturing, paint, pesticide, petroleum purifying … etc.; tends to accumulate heavy metals in living organisms causing disordering and diseases to the non-biodegradability of heavy metals of water pollutants. Lead, zinc, cadmium, chromium, copper, arsenic, and mercury are among these hazardous heavy metals even their existence in trace amounts in soil also causes problems [1].

Scientists were challenged to explore low-cost and environmentally friendly methods for heavy metals removal from wastewater [97]. Adsorption is considered an effective process for the elimination of environmental pollutants from aqueous solutions such as heavy metals. The main properties of the adsorbent materials are high thermal stability and erosion resistance besides small pore size, which results in higher exposed surface area and hence high adsorption capacity.

Polymer-polymer composites act as an efficient physical block for metal removal from aquatic streams. Furthermore, polymer-polymer composites are characterized by the high availability of improving adsorptive efficiency via crosslinking, blending, and surface functionalization [98].

The mechanism of metal ions capture via membranes could be assumed as its capability performance as a physical barrier for pollutant removal. Additionally, the metal ions may be eliminated through chemical adsorption through electrostatic interaction, complex formation, or hydrogen bonding as the composite displayed functional groups i.e., hydroxyl, amino, or carboxyl groups. The adsorption mechanism is based on sources, structures, the adsorbate and adsorbent natures, as well as attraction forces. During the chemisorption mechanism ionic exchanging, electrostatic interaction, reduction/oxidation interaction, and/or complexation (chelation) formation were involved based on the functional groups within the structure blocks of the adsorbent which controls how the adsorption processing takes place [99].

In other words, Polymeric NFMs can potentially improve the adsorption performance owing to their large surface area, high porosity, and small pore sizes, which provide a large number of potential active adsorption sites [100]. Hydroxyl and amino groups of Ch are very effective in the adsorption of toxic metal ions by electrostatic interactions [101]. Furthermore, the incorporation of Ch into the electro-spun nano-fibrous membrane has been successfully applied for several heavy metal removal [102].

Table 6 presented the removal capacity of the prepared PAN, PA, PA -1.25%Ch for Cu^{+2}, Cr^{+3}, and Pb^{+2} after different contact times.

Results in Table 6 show the higher metal cations sorption capacity of PA-1.25%Ch-NFs and PAN/PA-1.25%Ch-DLNFs compared with PAN or PA. This is owing to the presence of the amino ($–NH_2$) and hydroxyl (–OH) groups, especially in the C-3 position, in Ch that are responsible for the metal cations capturing through the chelation mechanism. Moreover, at pH close to neutrality (or weak acidity), the free electron pairs on the nitrogen of amino groups may bind metal cations via a chelation mechanism [103]. Similarly, as clear in Table 6, PA-NFs have a partial capacity to capture metal cations because of the presence of amino groups in their backbone structure.

The removal efficiency % of Cu^{+2}, Cr^{+3}, and Pb^{+2} by PAN/PA-1.25%Ch-DLNFs is relatively lower than that by PA -1.25%Ch-NFs.

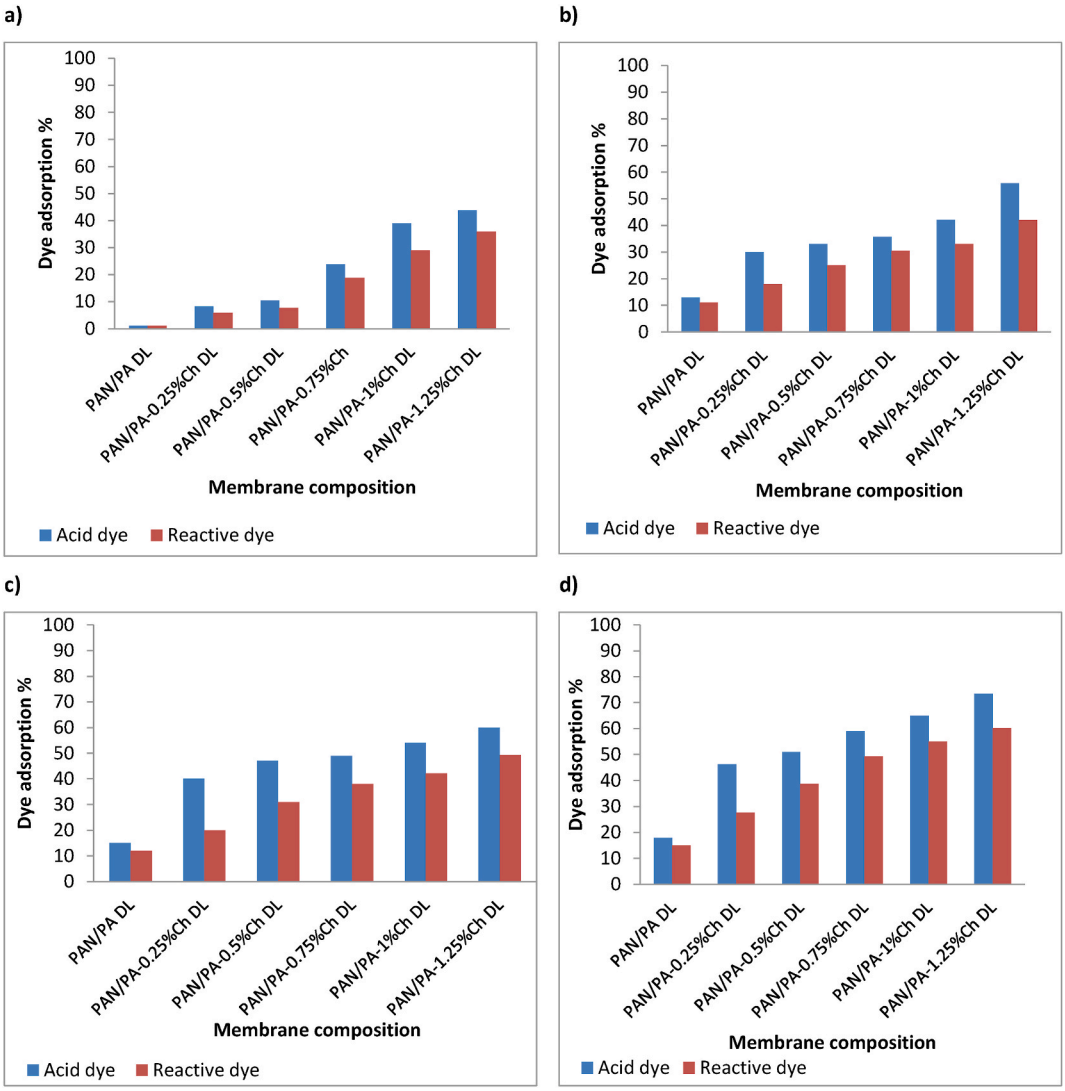

Fig. 14. Adsorption of anionic dyes (acid and reactive) by PAN, PA and PA/Ch-DLNFMs at room temperature after a) 1hr, b) 1day, c) 2 days and d) 3 days.

This can be explained by the presence of a PAN layer in the DLNFs membrane which has no active sites compared with PA/Ch-NFs. On the other hand, the diameter of the obtained NFs plays an important role in the sorption capacity of NFM. Reduction in fiber size and increase in surface porosity always leads to a membrane with a high surface area which is reflected in sorption capacity [104].

4. Conclusions

In this study, functional DLNFMs were prepared by electro-spinning of PAN and PA/Ch followed by hot-press under certain conditions. SEM clarifies that after hot-pressing, the two layers transport the fibers closer together resulting in smaller pores and a smoother surface by the formation of a much more regular structure with a stable dimensional network and reduced thickness which assisted in improving the mechanical properties of the obtained membrane. TGA of DLNFMs shows the decomposition temperature of the chitosan functionalized DLMs reached about 617 °C with a maximum weight loss of 60 % due to the presence of Ch polymer resulting in strengthening the produced bi-layered membrane to get the highest thermal stability compared with the other NFMs. Furthermore, the presence of both endo and exo thermic peaks of PA and PAN-NFs with slight shifting that these bi-layered NFs are physically bonded and hot-press steps do not strictly influence the thermal stability of these DLMs. Results of dye and heavy metal removal show the maximum removal efficiency of acid dyes reached 73.4 % and of reactive dye was approximately 61 % for PAN/PA-1.25%Ch DLNFM after 3 days at room temperature. The removal efficiency percent of heavy metal ions reached to 54 % by DLNFMs.

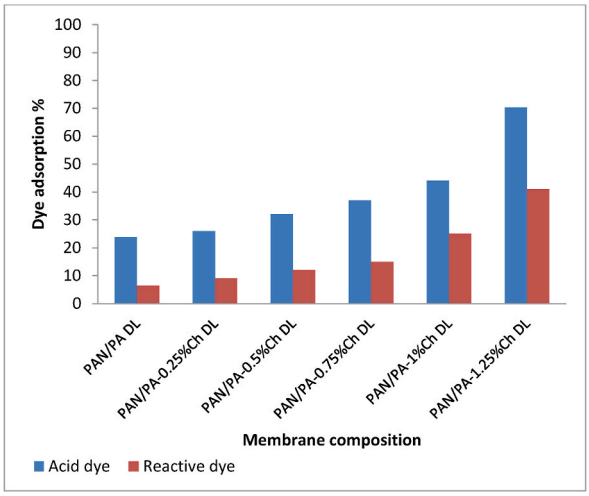

Fig. 15. Adsorption of anionic dyes (acid and reactive) by PAN, PA and PA/Ch-DLNFMs containing different amounts of Ch at 60 °C for 1hr.

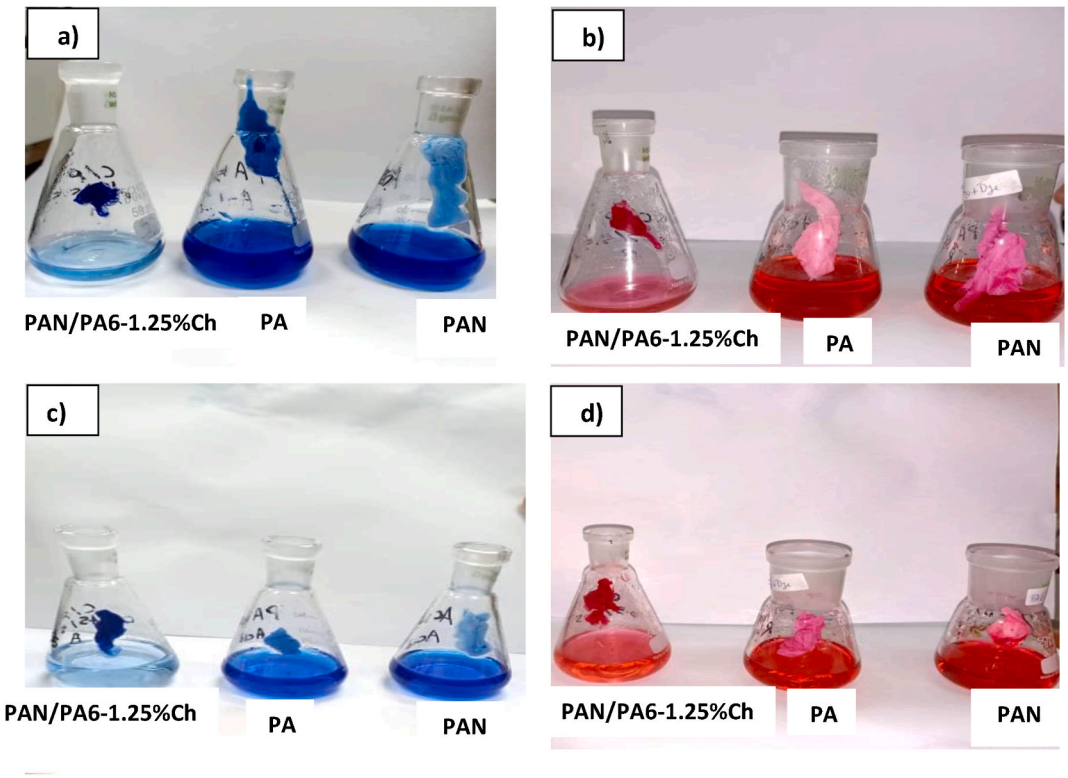

Fig. 16. Adsorption capacity of a) acid dye, b) reactive dye by DLNFs after 3 days at room temperature and c) acid dye, d) reactive dye by DLNFs after 1hr at 60 °C.

CRediT authorship contribution statement

AmanyE. Taha: Funding acquisition. **Salwa Mowafi:** Supervision. **Asmaa S. Hamouda:** Supervision.

Declaration of competing interest

The authors declare the following financial interests/personal relationships that may be considered potential competing interests: Amany. E. Taha reports financial support was provided by the Academy of Scientific Research and Technology (ASRT), Egypt. If there

Table 6
Removal efficiency (%) of metal cations by the prepared NFMs after different contact times at room temperature.

Metal Cation	Contact time (h)	Removal efficiency %			
		PAN-NFs	PA-NFs	PA -1.25%Ch NFs	PAN/PA-1.25 % Ch DLNFs
Cu^{+2}	2	3.2	10.2	22.1	20
	24	4.7	19.6	39.8	35.3
	48	5.6	30.9	45.8	41.6
	72	6.7	33.3	62.4	55.8
Cr^{+3}	2	2.1	11.6	23.5	20.4
	24	3.2	20.8	35	30.8
	48	5.3	29.2	43	41.9
	72	5.4	31.3	60.2	54.5
Pb^{+2}	2	2	13.3	22.2	19.2
	24	3.1	18.3	38.3	33.2
	48	4.8	23.5	48.4	38.4
	72	5.3	31.6	62.5	52.4

are other authors, they declare that they have no known competing financial interests or personal relationships that could have appeared to influence the work reported in this paper.

Acknowledgments

We are very grateful to the Academy of Scientific Research and Technology (ASRT), Egypt, for the Scientists of Next Generation (SNG) scholarship cycle six to achieve this work.

References

[1] N. Abdullah, N. Yusof, W.J. Lau, J. Jaafar, A.F. Ismail, "Recent trends of heavy metal removal from water/wastewater by membrane technologies,", J. Ind. Eng. Chem. 76 (2019) 17–38.
[2] S. Mowafi, M. Abou Taleb, H. El-Sayed, "NOZZLELESS ELECTROSPUN NANOFIBERS for remediation of textile wastewater,", Nanosci. Technol. An Int. J. 13 (no. 1) (2022).
[3] M. Amini, M. Arami, N.M. Mahmoodi, A. Akbari, "Dye removal from colored textile wastewater using acrylic grafted nanomembrane," Desalination, vol, 267, no 1 (2011) 107–113.
[4] M.A. Shannon, P.W. Bohn, M. Elimelech, J.G. Georgiadis, B.J. Marinas, A.M. Mayes, "Science and technology for water purification in the coming decades, Nature 452 (2008) 301e310.
[5] Z.F. Cui, H.S. Muralidhara, Membrane Technology: a Practical Guide to Membrane Technology and Applications in Food and Bioprocessing, Elsevier, 2010.
[6] N.L. Le, S.P. Nunes, "Materials and membrane technologies for water and energy sustainability,", Sustain. Mater. Technol. 7 (2016) 1–28.
[7] A. Razmjou, E. Arifin, G. Dong, J. Mansouri, V. Chen, "Superhydrophobic modification of TiO2 nanocomposite PVDF membranes for applications in membrane distillation,", J. Membr. Sci. 415 (2012) 850–863.
[8] J. Zhang, Z. Song, B. Li, Q. Wang, S. Wang, "Fabrication and characterization of superhydrophobic poly (vinylidene fluoride) membrane for direct contact membrane distillation," Desalination, 324 (2013) 1–9.
[9] S. Wu, W. Shi, L. Cui, C. Xu, "Enhancing contaminant rejection efficiency with ZIF-8 molecular sieving in sustainable mixed matrix membranes,", Chem. Eng. J. 482 (2024) 148954.
[10] W. Shi, C. Xu, J. Cai, S. Wu, "Advancements in material selection and application research for mixed matrix membranes in water treatment,", J. Environ. Chem. Eng. (2023) 111292.
[11] S. Wu, et al., "Chitosan-based hollow nanofiber membranes with polyvinylpyrrolidone and polyvinyl alcohol for efficient removal and filtration of organic dyes and heavy metals,", Int. J. Biol. Macromol. 239 (2023) 124264.
[12] S. Wu, K. Li, W. Shi, J. Cai, "Preparation and performance evaluation of chitosan/polyvinylpyrrolidone/polyvinyl alcohol electrospun nanofiber membrane for heavy metal ions and organic pollutants removal,", Int. J. Biol. Macromol. 210 (2022) 76–84.
[13] G. Nallathambi, D. Baskar, A.K. Selvam, "Preparation and characterization of triple layer membrane for water filtration," Environ. Sci. Pollut. Res., vol, 27, no 24 (2020) 29717–29724.
[14] G. Nallathambi, D. Baskar, A.K. Selvam, "Preparation and characterization of triple layer membrane for water filtration," Environ. Sci. Pollut. Res., vol, 27, no 24 (2020) 29717–29724, https://doi.org/10.1007/s11356-019-06254-z.
[15] S. Mowafi, H. El-Sayed, "Production and utilization of keratin and sericin-based electro-spun nanofibers: a comprehensive review," J. Nat. Fibers, vol, 20, no 1 (2023) 2192544.
[16] N. Bhardwaj, S.C. Kundu, "Electrospinning: a fascinating fiber fabrication technique," Biotechnol. Adv., vol, 28, no 3 (2010) 325–347.
[17] M. Rahman, A.M. Asiri, Nanofiber research: reaching new heights, Intech (2016) [Online]. Available, https://books.google.com.eg/books?id=asGQDwAAQBAJ.
[18] W. Kang, et al., "Sulfur-embedded porous carbon nanofiber composites for high stability lithium-sulfur batteries,", Chem. Eng. J. 333 (2018) 185–190.
[19] V. Guarino, I. Bonadies, L. Ambrosio, "Fabrication of Nanofibers and Nanotubes for Tissue Regeneration and Repair," in Peptides and Proteins as Biomaterials for Tissue Regeneration and Repair, Elsevier, 2018, pp. 205–228.
[20] M.A. Daniele, D.A. Boyd, A.A. Adams, F.S. Ligler, "Microfluidic strategies for design and assembly of microfibers and nanofibers with tissue engineering and regenerative medicine applications," Adv. Healthc. Mater., vol, 4, no 1 (2015) 11–28.
[21] S. Kailasa, M.S.B. Reddy, M.R. Maurya, B.G. Rani, K.V. Rao, K.K. Sadasivuni, "Electrospun nanofibers: materials, synthesis parameters, and their role in sensing applications," Macromol. Mater. Eng., vol, 306, no 11 (2021) 2100410.
[22] M.O. Guerrero-Pérez, "Research progress on the applications of electrospun nanofibers in catalysis," Catalysts, vol, 12, no 1 (2021) 9.
[23] M.H. Kim, et al., "Development of nanofiber reinforced double layered cabin air filter using novel upward mass production electrospinning set up," J. Nanosci. Nanotechnol., vol, 18, no 3 (2018) 2132–2136.
[24] A. Karczewski, et al., "Clindamycin-modified triple antibiotic nanofibers: a stain-free antimicrobial intracanal drug delivery system," J. Endod., vol, 44, no 1 (2018) 155–162.
[25] M.K. Sinha, B.R. Das, K. Kumar, B. Kishore, N.E. Prasad, "Development of Ultraviolet (UV) radiation protective fabric using combined electrospinning and electrospraying technique," J. Inst. Eng. Ser. E, vol, 98, no 1 (2017) 17–24.

[26] X. Pan, M. Fantin, F. Yuan, K. Matyjaszewski, "Externally controlled atom transfer radical polymerization," Chem. Soc. Rev., vol, 47, no 14 (2018) 5457–5490.
[27] D.A. Musale, A. Kumar, G. Pleizier, "Formation and characterization of poly (acrylonitrile)/chitosan composite ultrafiltration membranes," J. Memb. Sci., vol, 154, no 2 (1999) 163–173.
[28] D.A. Musale, A. Kumar, "Solvent and pH resistance of surface crosslinked chitosan/poly (acrylonitrile) composite nanofiltration membranes," J. Appl. Polym. Sci., vol, 77, no 8 (2000) 1782–1793.
[29] M.V. Chandorikar, P.C. Bhavsar, "Evaluation of polyacrylonitrile and poly (methyl methacrylate) as membrane materials for reverse-osmosis,", Indian J. Technol. 21 (3) (1983) 124–125. COUNCIL SCIENTIFIC INDUSTRIAL RESEARCH PUBL & INFO DIRECTORATE, NEW DELHI.
[30] H.M. Manohara, S.S. Nayak, G. Franklin, S.K. Nataraj, D. Mondal, "Progress in marine derived renewable functional materials and biochar for sustainable water purification,", Green Chem. (2021).
[31] J.R. Dodson, et al., "Bio-derived materials as a green route for precious & critical metal recovery and re-use," Green Chem., vol, 17, no 4 (2015) 1951–1965.
[32] D.A. Musale, A. Kumar, "Effects of surface crosslinking on sieving characteristics of chitosan/poly (acrylonitrile) composite nanofiltration membranes,", Sep. Purif. Technol. 21 (1–2) (2000) 27–37.
[33] Q. Long, Z. Zhang, G. Qi, Z. Wang, Y. Chen, Z.-Q. Liu, "Fabrication of chitosan nanofiltration membranes by the film casting strategy for effective removal of dyes/salts in textile wastewater," ACS Sustain. Chem. Eng., vol, 8, no 6 (2020) 2512–2522.
[34] S. Chatterjee, H.N. Tran, O.-B. Godfred, S.H. Woo, "Supersorption capacity of anionic dye by newer chitosan hydrogel capsules via green surfactant exchange method," ACS Sustain. Chem. Eng., vol, 6, no 3 (2018) 3604–3614.
[35] S. Jana, A. Saikia, M.K. Purkait, K. Mohanty, "Chitosan based ceramic ultrafiltration membrane: preparation, characterization and application to remove Hg (II) and as (III) using polymer enhanced ultrafiltration," Chem. Eng. J., vol, 170, no 1 (2011) 209–219.
[36] S. Wu, K. Li, W. Shi, J. Cai, "Chitosan/polyvinylpyrrolidone/polyvinyl alcohol/carbon nanotubes dual layers nanofibrous membrane constructed by electrospinning-electrospray for water purification," Carbohydr, Polymers 294 (2022) 119756.
[37] P. Gharbani, A. Mehrizad, "Preparation and characterization of graphitic carbon nitrides/polyvinylidene fluoride adsorptive membrane modified with chitosan for Rhodamine B dye removal from water: adsorption isotherms, kinetics and thermodynamics,", Carbohydr. Polym. 277 (2022) 118860.
[38] M.-X. Huo, Y.-L. Jin, Z.-F. Sun, F. Ren, L. Pei, P.-G. Ren, "Facile synthesis of chitosan-based acid-resistant composite films for efficient selective adsorption properties towards anionic dyes,", Carbohydr. Polym. 254 (2021) 117473.
[39] F. Yalcinkaya, B. Yalcinkaya, J. Hruza, "Electrospun polyamide-6 nanofiber hybrid membranes for wastewater treatment,", Fibers Polym. 20 (1) (2019) 93–99.
[40] W. Yang, R. Li, C. Fang, W. Hao, "Surface modification of polyamide nanofiber membranes by polyurethane to simultaneously improve their mechanical strength and hydrophobicity for breathable and waterproof applications,", Prog. Org. Coating 131 (2019) 67–72.
[41] Q.-C. Xia, M.-L. Liu, X.-L. Cao, Y. Wang, W. Xing, S.-P. Sun, "Structure design and applications of dual-layer polymeric membranes,", J. Membr. Sci. 562 (2018) 85–111.
[42] I.U. Khan, et al., "Status and improvement of dual-layer hollow fiber membranes via co-extrusion process for gas separation: a review,", J. Nat. Gas Sci. Eng. 52 (2018) 215–234.
[43] E. Tohidian, A. Dehban, F.Z. Ashtiani, A. Kargari, "Fabrication and characterization of a cross-linked two-layer polyetherimide solvent-resistant ultrafiltration (SRUF) membrane for separation of toluene–water mixture,", Chem. Eng. Res. Des. 168 (2021) 59–70.
[44] Z.-Y. Wang, et al., "Designing scalable dual-layer composite hollow fiber nanofiltration membranes with fully cross-linked ultrathin functional layer,", J. Membr. Sci. 628 (2021) 119243.
[45] Z. Fu, et al., "Dual-layer membrane with hierarchical hydrophobicity and transport channels for nonpolar organic solvent nanofiltration,", AIChE J. 67 (4) (2021) e17138.
[46] F.-J. Fu, S.-P. Sun, S. Zhang, T.-S. Chung, "Pressure retarded osmosis dual-layer hollow fiber membranes developed by co-casting method and ammonium persulfate (APS) treatment,", J. Membr. Sci. 469 (2014) 488–498.
[47] Y.C. Woo, et al., "Electrospun dual-layer nonwoven membrane for desalination by air gap membrane distillation,", Desalination 403 (2017) 187–198.
[48] Y. Wang, T.S. Chung, B.W. Neo, M. Gruender, "Processing and engineering of pervaporation dehydration of ethylene glycol via dual-layer polybenzimidazole (PBI)/polyetherimide (PEI) membranes,", J. Membr. Sci. 378 (1–2) (2011) 339–350.
[49] H. Dzinun, M.H.D. Othman, A.F. Ismail, M.H. Puteh, M.A. Rahman, J. Jaafar, "Fabrication of dual layer hollow fibre membranes for photocatalytic degradation of organic pollutants,", Int. J. Chem. Eng. Appl 6 (4) (2015) 289.
[50] S. Mowafi, M. Abou Taleb, C. Vineis, H. El-Sayed, "Structure [1] S. Mowafi, M. Abou Taleb, C. Vineis, and H. El-Sayed, 'Structure and potential applications of polyamide 6/protein electro-spun nanofibrous mats in sorption of metal ions and dyes from industrial effluents,', J. Appl. Res. Technol. 19 (4) (2021) 322–335, vol. 19, ," J. Appl. Res. Technol.
[51] S. Mowafi, H.-A.S. Tohamy, "Application of electro-spun nano-fibers based on agriculture cellulosic biomaterial wastes for removal of dye and heavy metal from polluted water,", J. Text. Inst. (2023) 1–10.
[52] S. Shang, F. Yang, X. Cheng, X.F. Walboomers, J.A. Jansen, "The Effect of Electrospun Fibre Alignment on the Behaviour of Rat Periodontal Ligament cells.,", 2010.
[53] F. Yalcinkaya, "Preparation of various nanofiber layers using wire electrospinning system,", Arab. J. Chem. 12 (8) (2019) 5162–5172.
[54] T. Kozior, A. Mamun, M. Trabelsi, M. Wortmann, S. Lilia, A. Ehrmann, "Electrospinning on 3D printed polymers for mechanically stabilized filter composites,", Polymers 11 (12) (2019) 2034.
[55] B.D. Ippel, E.E. Van Haaften, C.V.C. Bouten, P.Y.W. Dankers, "Impact of additives on mechanical properties of supramolecular electrospun scaffolds,", ACS Appl. Polym. Mater. 2 (9) (2020) 3742–3748.
[56] H. Kurita, R. Ishigami, C. Wu, F. Narita, "Mechanical properties of mechanically-defibrated cellulose nanofiber reinforced epoxy resin matrix composites,", J. Compos. Mater. 55 (4) (2021) 455–464.
[57] L. Sabantina, et al., "Fixing PAN nanofiber mats during stabilization for carbonization and creating novel metal/carbon composites,", Polymers 10 (7) (2018) 735.
[58] P. Chavoshnejad, M.J. Razavi, "Effect of the interfiber bonding on the mechanical behavior of electrospun fibrous mats,", Sci. Rep. 10 (1) (2020) 7709.
[59] E. Wirth, L. Sabantina, M.O. Weber, K. Finsterbusch, A. Ehrmann, "Preliminary study of ultrasonic welding as a joining process for electrospun nanofiber mats,", Nanomaterials 8 (10) (2018) 746.
[60] J. Nasser, J. Lin, K. Steinke, H.A. Sodano, "Enhanced interfacial strength of aramid fiber reinforced composites through adsorbed aramid nanofiber coatings,", Compos. Sci. Technol. 174 (2019) 125–133.
[61] F. Yalcinkaya, J. Hruza, "Effect of laminating pressure on polymeric multilayer nanofibrous membranes for liquid filtration,", Nanomaterials 8 (5) (2018) 272.
[62] R. Roche, F. Yalcinkaya, "Incorporation of PVDF nanofibre multilayers into functional structure for filtration applications,", Nanomaterials 8 (10) (2018) 771.
[63] P. Ginestra, E. Ceretti, A. Fiorentino, "Electrospinning of poly-caprolactone for scaffold manufacturing: experimental investigation on the process parameters influence,", Procedia CIRP 49 (2016) 8–13.
[64] A. Luzio, E.V. Canesi, C. Bertarelli, M. Caironi, "Electrospun polymer fibers for electronic applications,", Materials 7 (2) (2014) 906–947.
[65] T.J. Sill, H.A. Von Recum, "Electrospinning: applications in drug delivery and tissue engineering,", Biomaterials 29 (13) (2008) 1989–2006.
[66] Q.P. Pham, U. Sharma, A.G. Mikos, "Electrospun poly (ε-caprolactone) microfiber and multilayer nanofiber/microfiber scaffolds: characterization of scaffolds and measurement of cellular infiltration,", Biomacromolecules 7 (10) (2006) 2796–2805.
[67] H.M. Golecki, et al., "Effect of solvent evaporation on fiber morphology in rotary jet spinning,", Langmuir 30 (44) (2014) 13369–13374.
[68] N. Charernsriwilaiwat, P. Opanasopit, T. Rojanarata, T. Ngawhirunpat, P. Supaphol, "Preparation and characterization of chitosan-hydroxybenzotriazole/polyvinyl alcohol blend nanofibers by the electrospinning technique,", Carbohydr. Polym. 81 (3) (2010) 675–680.
[69] Y. Liu, R. Wang, H. Ma, B.S. Hsiao, B. Chu, "High-flux microfiltration filters based on electrospun polyvinylalcohol nanofibrous membranes,", Polymer (Guildf). 54 (2) (2013) 548–556.

[70] Ç. Akduman, "PVDF electrospun nanofiber membranes for microfiltration: the effect of pore size and thickness on membrane performance,", Avrupa Bilim ve Teknol. Derg. (16) (2019) 247–255.
[71] B.S. Lalia, E. Guillen-Burrieza, H.A. Arafat, R. Hashaikeh, "Fabrication and characterization of polyvinylidenefluoride-co-hexafluoropropylene (PVDF-HFP) electrospun membranes for direct contact membrane distillation,", J. Membr. Sci. 428 (2013) 104–115.
[72] C.K. Kundu, X. Wang, M.Z. Rahman, L. Song, Y. Hu, "Application of chitosan and DOPO derivatives in fire protection of polyamide 66 textiles: towards a combined gas phase and condensed phase activity,", Polym. Degrad. Stabil. 176 (2020) 109158.
[73] B.K. Shrestha, H.M. Mousa, A.P. Tiwari, S.W. Ko, C.H. Park, C.S. Kim, "Development of polyamide-6, 6/chitosan electrospun hybrid nanofibrous scaffolds for tissue engineering application,", Carbohydr. Polym. 148 (2016) 107–114.
[74] X. Yang, et al., "Electrospun polymer composite membrane with superior thermal stability and excellent chemical resistance for high-efficiency PM2. 5 capture,", ACS Appl. Mater. Interfaces 11 (46) (2019) 43188–43199.
[75] S.D. Ghodke, A.B. Tamboli, A. V Diwate, V.P. Ubale, N.N. Maldar, "Synthesis, characterization and properties of novel polyamides derived from 4 4' bis (4-carboxy methylene) biphenyl and various diamines,", Des. Monomers Polym. 23 (1) (2020) 177–187.
[76] Z. Song, X. Hou, L. Zhang, S. Wu, "Enhancing crystallinity and orientation by hot-stretching to improve the mechanical properties of electrospun partially aligned polyacrylonitrile (PAN) nanocomposites,", Materials 4 (4) (2011) 621–632.
[77] W.S. Khan, "Chemical and thermal investigations of electrospun polyacrylonitrile nanofibers incorporated with various nanoscale inclusions,", J. Therm. Eng. 3 (4) (2017) 1375–1390.
[78] Y. Ma, T. Zhou, C. Zhao, "Preparation of chitosan–nylon-6 blended membranes containing silver ions as antibacterial materials,", Carbohydr. Res. 343 (2) (2008) 230–237.
[79] T.M. Majka, M. Cokot, K. Pielichowski, "Studies on the thermal properties and flammability of polyamide 6 nanocomposites surface-modified via layer-by-layer deposition of chitosan and montmorillonite,", J. Therm. Anal. Calorim. 131 (2018) 405–416.
[80] S. Adibzadeh, S. Bazgir, A.A. Katbab, "Fabrication and characterization of chitosan/poly (vinyl alcohol) electrospun nanofibrous membranes containing silver nanoparticles for antibacterial water filtration,", Iran. Polym. J. (Engl. Ed.) 23 (2014) 645–654.
[81] V. González, C. Guerrero, U. Ortiz, "Chemical structure and compatibility of polyamide–chitin and chitosan blends,", J. Appl. Polym. Sci. 78 (4) (2000) 850–857.
[82] Z. Zakaria, Z. Izzah, M. Jawaid, A. Hassan, "Effect of degree of deacetylation of chitosan on thermal stability and compatibility of chitosan-polyamide blend.,", Bioresources 7 (4) (2012).
[83] O. Eren, N. Ucar, A. Onen, N. Kizildag, I. Karacan, "Synergistic effect of polyaniline, nanosilver, and carbon nanotube mixtures on the structure and properties of polyacrylonitrile composite nanofiber,", J. Compos. Mater. 50 (15) (2016) 2073–2086.
[84] H.S. Mahmood, M.K. Jawad, "Antibacterial activity of chitosan/PAN blend prepared at different ratios,", in: AIP Conference Proceedings, vol. 2190, 2019 no. 1.
[85] C. Wang, W. Wang, L. Zhang, S. Zhong, D. Yu, "Electrospinning of PAN/Ag NPs nanofiber membrane with antibacterial properties,", J. Mater. Res. 34 (10) (2019) 1669–1677.
[86] B.S. Metwally, S.A. Rashed, M.N. El-Sheikh, A.S. Hamouda, "Dyeing of recycled electrospun polyamide 6 nanofibers: implications of dye particle size,", Fibers Polym. 24 (5) (2023) 1681–1693.
[87] G.L. Dotto, et al., "Chitosan/polyamide nanofibers prepared by Forcespinning® technology: a new adsorbent to remove anionic dyes from aqueous solutions,", J. Clean. Prod. 144 (2017) 120–129.
[88] M. Fazeli, F. Fazeli, T. Nuge, O. Abdoli, S. Moghaddam, "Study on the preparation and properties of polyamide/chitosan nanocomposite fabricated by electrospinning method,", J. Polym. Environ. (2022) 1–9.
[89] S. Nauman, G. Lubineau, H.F. Alharbi, "Post processing strategies for the enhancement of mechanical properties of enms (Electrospun nanofibrous membranes): a review,", Membranes 11 (1) (2021) 39.
[90] Y.-Q. Liu, J.-W. Feng, C.-C. Zhang, Y. Teng, Z. Liu, J.-H. He, "Air permeability of nanofiber membrane with hierarchical structure,", Therm. Sci. 22 (4) (2018) 1637–1643.
[91] R. Roche, F. Yalcinkaya, "Electrospun polyacrylonitrile nanofibrous membranes for point-of-use water and air cleaning,", ChemistryOpen 8 (1) (2019) 97–103.
[92] M.N. Islam, B. Yıldırım, J. Maryska, F. Yalcinkaya, "Multi-layered nanofiber membranes: preparation, characterization, and application in wastewater treatment,", J. Ind. Text. 52 (2022) 15280837221127444.
[93] V. Pais, C. Mota, J. Bessa, J.G. Dias, F. Cunha, R. Fangueiro, "Study of the filtration performance of multilayer and multiscale fibrous structures,", Materials 14 (23) (2021) 7147.
[94] A. Tcharkhtchi, N. Abbasnezhad, M.Z. Seydani, N. Zirak, S. Farzaneh, M. Shirinbayan, "An overview of filtration efficiency through the masks: mechanisms of the aerosols penetration,", Bioact. Mater. 6 (1) (2021) 106–122.
[95] M. Ghani, A.A. Gharehaghaji, M. Arami, N. Takhtkuse, B. Rezaei, "Fabrication of electrospun polyamide-6/chitosan nanofibrous membrane toward anionic dyes removal,", J. Nanotechnol (2014) 2014.
[96] H. Zhang, et al., "Elaboration, characterization and study of a novel affinity membrane made from electrospun hybrid chitosan/nylon-6 nanofibers for papain purification,", J. Mater. Sci. 45 (2010) 2296–2304.
[97] A.Y. Abdolmaleki, H. Zilouei, S.N. Khorasani, "Characterization of electrospinning parameters of chitosan/poly (vinyl alcohol) nanofibers to remove phenol via response surface methodology,", Polym. Sci. 4 (2018) 1–9.
[98] R. Zhang, Y. Zhou, X. Gu, J. Lu, "Competitive adsorption of methylene blue and Cu2+ onto citric acid modified pine sawdust,", Clean: Soil, Air, Water 43 (1) (2015) 96–103.
[99] B. Nayak, A. Samant, R. Patel, P.K. Misra, "Comprehensive understanding of the kinetics and mechanism of fluoride removal over a potent nanocrystalline hydroxyapatite surface,", ACS Omega 2 (11) (2017) 8118–8128.
[100] H.F. Alharbi, M.Y. Haddad, M.O. Aijaz, A.K. Assaifan, M.R. Karim, "Electrospun bilayer PAN/chitosan nanofiber membranes incorporated with metal oxide nanoparticles for heavy metal ion adsorption,", Coatings 10 (3) (2020) 285.
[101] N. He, L. Li, P. Wang, J. Zhang, J. Chen, J. Zhao, "Dioxide/Chitosan/poly (lactide-co-caprolactone) composite membrane with efficient Cu (II) adsorption,", Colloids Surfaces A Physicochem. Eng. Asp 580 (2019) 123687.
[102] A. Kakoria, S. Sinha-Ray, S. Sinha-Ray, "Industrially scalable Chitosan/Nylon-6 (CS/N) nanofiber-based reusable adsorbent for efficient removal of heavy metal from water,", Polymer (Guildf). 213 (2021) 123333.
[103] E. Guibal, "Interactions of metal ions with chitosan-based sorbents: a review,", Sep. Purif. Technol. 38 (1) (2004) 43–74.
[104] K.C. Khulbe, T. Matsuura, "Removal of heavy metals and pollutants by membrane adsorption techniques,", Appl. Water Sci. 8 (2018) 1–30.